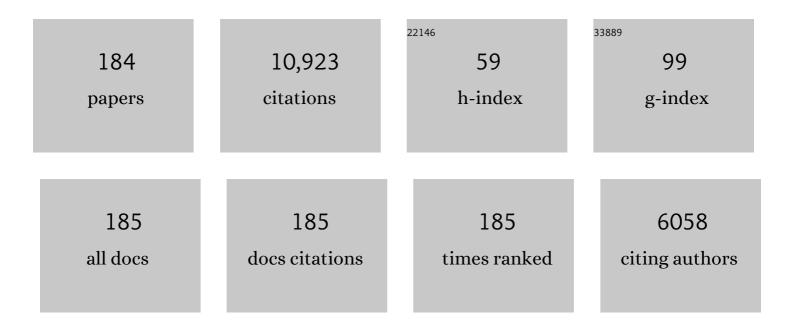
Robert A Creaser

List of Publications by Year in descending order

Source: https://exaly.com/author-pdf/6067069/publications.pdf Version: 2024-02-01



#	Article	IF	CITATIONS
1	A Whiff of Oxygen Before the Great Oxidation Event?. Science, 2007, 317, 1903-1906.	12.6	822
2	A-type granites revisited: Assessment of a residual-source model. Geology, 1991, 19, 163.	4.4	686
3	Cretaceous oceanic anoxic event 2 triggered by a massive magmatic episode. Nature, 2008, 454, 323-326.	27.8	398
4	Re-Os geochronology of postglacial black shales in Australia: Constraints on the timing of "Sturtian― glaciation. Geology, 2006, 34, 729.	4.4	250
5	Isotopic evidence for geochemical decoupling between ancient epeiric seas and bordering oceans: Implications for secular curves. Geology, 1998, 26, 567.	4.4	247
6	Macroscale NTIMS and microscale LA-MC-ICP-MS Re-Os isotopic analysis of molybdenite: Testing spatial restrictions for reliable Re-Os age determinations, and implications for the decoupling of Re and Os within molybdenite. Geochimica Et Cosmochimica Acta, 2004, 68, 3897-3908.	3.9	234
7	Re–Os geochronology of organic rich sediments: an evaluation of organic matter analysis methods. Chemical Geology, 2003, 200, 225-240.	3.3	232
8	Re-Os Geochronology and Systematics in Molybdenite from the Endako Porphyry Molybdenum Deposit, British Columbia, Canada. Economic Geology, 2001, 96, 197-204.	3.8	223
9	Uranium and molybdenum isotope evidence for an episode of widespread ocean oxygenation during the late Ediacaran Period. Geochimica Et Cosmochimica Acta, 2015, 156, 173-193.	3.9	222
10	Re–Os and Mo isotope systematics of black shales from the Middle Proterozoic Velkerri and Wollogorang Formations, McArthur Basin, northern Australia. Geochimica Et Cosmochimica Acta, 2009, 73, 2534-2558.	3.9	209
11	The temporal evolution of North American kimberlites. Lithos, 2004, 76, 377-397.	1.4	198
12	Timing of Iron Oxide Cu-Au-(U) Hydrothermal Activity and Nd Isotope Constraints on Metal Sources in the Gawler Craton, South Australia. Economic Geology, 2007, 102, 1441-1470.	3.8	172
13	Direct Radiometric Dating of Hydrocarbon Deposits Using Rhenium-Osmium Isotopes. Science, 2005, 308, 1293-1295.	12.6	168
14	Constraints on the timing of Marinoan "Snowball Earth―glaciation by 187Re–187Os dating of a Neoproterozoic, post-glacial black shale in Western Canada. Earth and Planetary Science Letters, 2004, 222, 729-740.	4.4	155
15	Assessment of the 187Re decay constant by cross calibration of Re–Os molybdenite and U–Pb zircon chronometers in magmatic ore systems. Geochimica Et Cosmochimica Acta, 2007, 71, 1999-2013.	3.9	153
16	U–Pb zircon dating by laser ablation-MC-ICP-MS using a new multiple ion counting Faraday collector array. Journal of Analytical Atomic Spectrometry, 2005, 20, 677.	3.0	149
17	Precise age of Bangiomorpha pubescens dates the origin of eukaryotic photosynthesis. Geology, 2018, 46, 135-138.	4.4	148
18	Further evaluation of the Re-Os geochronometer in organic-rich sedimentary rocks: a test of hydrocarbon maturation effects in the Exshaw Formation, Western Canada Sedimentary Basin. Geochimica Et Cosmochimica Acta, 2002, 66, 3441-3452.	3.9	140

#	Article	IF	CITATIONS
19	Macrocrystal phlogopite Rb–Sr dates for the Ekati property kimberlites, Slave Province, Canada: evidence for multiple intrusive episodes in the Paleocene and Eocene. Lithos, 2004, 76, 399-414.	1.4	136
20	Absolute timing of sulfide and gold mineralization: A comparison of Re-Os molybdenite and Ar-Ar mica methods from the Tintina Gold Belt, Alaska. Geology, 2002, 30, 791.	4.4	132
21	Age and source constraints for the giant Muruntau gold deposit, Uzbekistan, from coupled Re-Os-He isotopes in arsenopyrite. Geology, 2007, 35, 795.	4.4	126
22	The role of Indian and Tibetan lithosphere in spatial distribution of Cenozoic magmatism and porphyry Cu–Mo deposits in the Gangdese belt, southern Tibet. Earth-Science Reviews, 2015, 150, 68-94.	9.1	118
23	Standardizing Re–Os geochronology: A new molybdenite Reference Material (Henderson, USA) and the stoichiometry of Os salts. Chemical Geology, 2007, 244, 74-87.	3.3	116
24	Lu–Hf, in-situ Sr and Pb isotope and trace element systematics for mantle eclogites from the Diavik diamond mine: Evidence for Paleoproterozoic subduction beneath the Slave craton, Canada. Earth and Planetary Science Letters, 2007, 254, 55-68.	4.4	109
25	Investigating a child sacrifice event from the Inca heartland. Journal of Archaeological Science, 2011, 38, 323-333.	2.4	105
26	Re–Os elemental and isotopic systematics in crude oils. Geochimica Et Cosmochimica Acta, 2007, 71, 378-386.	3.9	104
27	Yardea Dacite—Large-volume, high-temperature felsic volcanism from the Middle Proterozoic of South Australia. Geology, 1991, 19, 48.	4.4	103
28	Direct radiometric dating of the Devonian-Mississippian time-scale boundary using the Re-Os black shale geochronometer. Geology, 2005, 33, 545.	4.4	103
29	Evaluation of bitumen as a Re–Os geochronometer for hydrocarbon maturation and migration: A test case from the Polaris MVT deposit, Canada. Earth and Planetary Science Letters, 2005, 235, 1-15.	4.4	100
30	Mineralogical constraints on the paleoenvironments of the Ediacaran Doushantuo Formation. Proceedings of the National Academy of Sciences of the United States of America, 2009, 106, 13190-13195.	7.1	100
31	No evidence for Hadean continental crust within Earth's oldest evolved rock unit. Nature Geoscience, 2016, 9, 777-780.	12.9	99
32	Migration in the Nile Valley during the New Kingdom period: a preliminary strontium isotope study. Journal of Archaeological Science, 2007, 34, 1391-1401.	2.4	94
33	Tectonomagmatic events during stretching and basin formation in the Labrador Sea and the Davis Strait: evidence from age and composition of Mesozoic to Palaeogene dyke swarms in West Greenland. Journal of the Geological Society, 2009, 166, 999-1012.	2.1	89
34	Multi-Stage Modification of the Northern Slave Mantle Lithosphere: Evidence from Zircon- and Diamond-Bearing Eclogite Xenoliths Entrained in Jericho Kimberlite, Canada. Journal of Petrology, 2006, 47, 821-858.	2.8	88
35	INâ€SITU ELEMENTAL AND Sr ISOTOPE INVESTIGATION OF HUMAN TOOTH ENAMEL BY LASER ABLATIONâ€(MC)â€ICPâ€MS: SUCCESSES AND PITFALLS*. Archaeometry, 2008, 50, 371-385.	1.3	88
36	Re-Os Sulfide Geochronology of the Red Dog Sediment-Hosted Zn-Pb-Ag Deposit, Brooks Range, Alaska. Economic Geology, 2004, 99, 1569-1576.	3.8	87

#	Article	IF	CITATIONS
37	Tectonic affinity of Nisutlin and Anvil assemblage strata from the Teslin tectonic zone, northern Canadian Cordillera: Constraints from neodymium isotope and geochemical evidence. Tectonics, 1997, 16, 107-121.	2.8	82
38	Preserved initial in apatite from altered felsic igneous rocks: A case study from the Middle Proterozoic of South Australia. Geochimica Et Cosmochimica Acta, 1992, 56, 2789-2795.	3.9	81
39	Timing of multiple hydrothermal events in the iron oxide–copper–gold deposits of the Southern Copper Belt, Carajás Province, Brazil. Mineralium Deposita, 2015, 50, 517-546.	4.1	81
40	Constraints on the genesis of gold mineralization at the Homestake Gold Deposit, Black Hills, South Dakota from rhenium–osmium sulfide geochronology. Mineralium Deposita, 2010, 45, 461-480.	4.1	75
41	North American margin origin of Quesnel terrane strata in the southern Canadian Cordillera: Inferences from geochemical and Nd isotopic characteristics of Triassic metasedimentary rocks. Bulletin of the Geological Society of America, 2002, 114, 462-475.	3.3	72
42	Sulphide survival and diamond genesis during formation and evolution of Archaean subcontinental lithosphere: A comparison between the Slave and Kaapvaal cratons. Lithos, 2009, 112, 747-757.	1.4	72
43	Zircon U–Pb age and Sr–Nd–Hf–O isotope geochemistry of the Paleocene–Eocene igneous rocks in western Gangdese: Evidence for the timing of Neo-Tethyan slab breakoff. Lithos, 2015, 224-225, 179-194.	1.4	71
44	Early and Middle Proterozoic evolution of Yukon, Canada. Canadian Journal of Earth Sciences, 2005, 42, 1045-1071.	1.3	70
45	Global correlation of the Vazante Group, São Francisco Basin, Brazil: Re–Os and U–Pb radiometric age constraints. Precambrian Research, 2008, 164, 160-172.	2.7	70
46	Elevated Magmatic Sulfur and Chlorine Contents in Ore-Forming Magmas at the Red Chris Porphyry Cu-Au Deposit, Northern British Columbia, Canada. Economic Geology, 2018, 113, 1047-1075.	3.8	70
47	Neoarchean and Paleoproterozoic Iron Oxide-Copper-Gold Events at the Sossego Deposit, Carajas Province, Brazil: Re-Os and U-Pb Geochronological Evidence. Economic Geology, 2015, 110, 809-835.	3.8	69
48	Early Mesoproterozoic intrusive breccias in Yukon, Canada: the role of hydrothermal systems in reconstructions of North America and Australia. Precambrian Research, 2001, 111, 31-55.	2.7	68
49	The Distribution and Timing of Molybdenite Mineralization at the El Teniente Cu-Mo Porphyry Deposit, Chile. Economic Geology, 2015, 110, 387-421.	3.8	68
50	Contrasting Tectonic Settings and Sulfur Contents of Magmas Associated with Cretaceous Porphyry Cu ± Mo ± Au and Intrusion-Related Iron Oxide Cu-Au Deposits in Northern Chile. Economic Geology, 2017, 112, 295-318.	3.8	68
51	Petrogenesis of a Mesoproterozoic quartz latite-granitoid suite from the Roxby Downs area, South Australia. Precambrian Research, 1996, 79, 371-394.	2.7	67
52	Queen Maud block: A newly recognized Paleoproterozoic (2.4–2.5 Ga) terrane in northwest Laurentia. Geology, 2007, 35, 707.	4.4	66
53	A model for the oceanic mass balance of rhenium and implications for the extent of Proterozoic ocean anoxia. Geochimica Et Cosmochimica Acta, 2018, 227, 75-95.	3.9	66
54	Rhenium-Osmium Geochronology of Arsenopyrite in Meguma Group Gold Deposits, Meguma Terrane, Nova Scotia, Canada: Evidence for Multiple Gold-Mineralizing Events. Economic Geology, 2005, 100, 1229-1242.	3.8	65

#	Article	IF	CITATIONS
55	¹⁸⁷ Re- ¹⁸⁷ Os geochronology of Precambrian organic-rich sedimentary rocks. Geological Society Special Publication, 2009, 326, 85-107.	1.3	65
56	Correlation of Sturtian diamictite successions in southern Australia and northwestern Tasmania by Re–Os black shale geochronology and the ambiguity of "Sturtian―type diamictite–cap carbonate pairs as chronostratigraphic marker horizons. Precambrian Research, 2009, 172, 301-310.	2.7	65
57	Geochronology and Geochemistry of the MAX Porphyry Mo Deposit and its Relationship to Pb-Zn-Ag Mineralization, Kootenay Arc, Southeastern British Columbia, Canada. Economic Geology, 2010, 105, 1113-1142.	3.8	64
58	Re–Os depositional ages and seawater Os estimates for the Frasnian–Famennian boundary: Implications for weathering rates, land plant evolution, and extinction mechanisms. Earth and Planetary Science Letters, 2007, 261, 649-661.	4.4	62
59	Transient episodes of mild environmental oxygenation and oxidative continental weathering during the late Archean. Science Advances, 2015, 1, e1500777.	10.3	61
60	Tectonic setting of the Taltson magmatic zone at 1.9–2.0 Ga: a granitoid-based perspective. Canadian Journal of Earth Sciences, 2000, 37, 1597-1609.	1.3	60
61	LATE AND MID-CRETACEOUS MINERALIZATION IN THE NORTHERN CANADIAN CORDILLERA: CONSTRAINTS FROM Re-Os MOLYBDENITE DATES. Economic Geology, 2001, 96, 1461-1467.	3.8	57
62	Age of the Zambian Copperbelt. Mineralium Deposita, 2017, 52, 1245-1268.	4.1	57
63	Formation of Paleoproterozoic eclogitic mantle, Slave Province (Canada): Insights from in-situ Hf and U–Pb isotopic analyses of mantle zircons. Earth and Planetary Science Letters, 2005, 240, 621-633.	4.4	56
64	Sulfide and whole rock Re–Os systematics of eclogite and pyroxenite xenoliths from the Slave Craton, Canada. Earth and Planetary Science Letters, 2009, 283, 48-58.	4.4	56
65	Discovery of pre-3.5 Ga exotic crust at the northwestern Superior Province margin, Manitoba. Geology, 2000, 28, 75.	4.4	54
66	Geochemical and Nd-Pb-O isotope systematics of granites from the Taltson Magmatic Zone, NE Alberta: implications for early Proterozoic tectonics in western Laurentia. Precambrian Research, 2000, 102, 221-249.	2.7	53
67	Hunter-gatherer mobility strategies and resource use based on strontium isotope (87Sr/86Sr) analysis: a case study from Middle Holocene Lake Baikal, Siberia. Journal of Archaeological Science, 2008, 35, 1265-1280.	2.4	51
68	Constraining the depositional history of the Neoproterozoic Shaler Supergroup, Amundsen Basin, NW Canada: Rhenium-osmium dating of black shales from the Wynniatt and Boot Inlet Formations. Precambrian Research, 2013, 236, 124-131.	2.7	51
69	Geochemistry and tectonic significance of alkalic mafic magmatism in the Yukon-Tanana terrane, Finlayson Lake region, Yukon. Canadian Journal of Earth Sciences, 2002, 39, 1729-1744.	1.3	50
70	Identifying foreigners versus locals in a burial population from Nasca, Peru: an investigation using strontium isotope analysis. Journal of Archaeological Science, 2009, 36, 2755-2764.	2.4	50
71	Neodymium isotopic constraints for the origin of Mesoproterozoic felsic magmatism, Gawler Craton, South Australia. Canadian Journal of Earth Sciences, 1995, 32, 460-471.	1.3	49
72	Extreme enrichment of high field strength elements in Jericho eclogite xenoliths: A cryptic record of Paleoproterozoic subduction, partial melting, and metasomatism beneath the Slave craton, Canada. Geology, 2002, 30, 507.	4.4	47

#	Article	IF	CITATIONS
73	Mid-Paleozoic initiation of the northern Cordilleran marginal backarc basin: Geologic, geochemical, and neodymium isotope evidence from the oldest mafic magmatic rocks in the Yukon-Tanana terrane, Finlayson Lake district, southeast Yukon, Canada. Bulletin of the Geological Society of America, 2004, 116, 1087.	3.3	45
74	Re-Os dating of pyrite confirms an early diagenetic onset and extended duration of mineralization in the Irish Zn-Pb ore field. Geology, 2015, 43, 143-146.	4.4	44
75	Re–Os and U–Pb geochronology of the Clear Creek, Dublin Gulch, and Mactung deposits, Tombstone Gold Belt, Yukon, Canada: absolute timing relationships between plutonism and mineralization. Canadian Journal of Earth Sciences, 2003, 40, 1839-1852.	1.3	43
76	Petrogenesis of the Cretaceous Cassiar batholith, Yukon-British Columbia, Canada: Implications for magmatism in the North American Cordilleran Interior. Bulletin of the Geological Society of America, 2000, 112, 1119-1133.	3.3	42
77	Temporal trends of pollution Pb and other metals in east-central Baffin Island inferred from lake sediment geochemistry. Science of the Total Environment, 2009, 407, 5653-5662.	8.0	42
78	Geochemical and Nd-Pb isotopic systematics of late Archean granitoids, southwestern Slave Province, Canada: constraints for granitoid origin and crustal isotopic structure. Canadian Journal of Earth Sciences, 1999, 36, 1131-1147.	1.3	40
79	Strontium isotope composition of runoff from a glaciated carbonate terrain. Geochimica Et Cosmochimica Acta, 2002, 66, 595-614.	3.9	39
80	Examining potential genetic links between Jurassic porphyry Cu–Au ± Mo and epithermal Au ±â mineralization in the Toodoggone district of North-Central British Columbia, Canada. Mineralium Deposita, 2009, 44, 463-496.	€‰Ag 4.1	39
81	Petrogenesis of the Late Cretaceous northern Alberta kimberlite province. Lithos, 2004, 76, 435-459.	1.4	37
82	Archean high-Mg monzodiorite–syenite, epidote skarn, and biotite–sericite gold lodes in the Granny Smith–Wallaby district, Australia: U–Pb and Re–Os chronometry of two intrusion-related hydrothermal systems. Mineralium Deposita, 2008, 43, 337-362.	4.1	36
83	Preâ€Alpine Crust in the Apuseni Mountains, Romania: Insights from Smâ€Nd and Uâ€Pb Data. Journal of Geology, 2002, 110, 341-354.	1.4	35
84	Mid- to late Paleozoic K-feldspar augen granitoids of the Yukon-Tanana terrane, Yukon, Canada: Implications for crustal growth and tectonic evolution of the northern Cordillera. Bulletin of the Geological Society of America, 2006, 118, 1212-1231.	3.3	34
85	Besshi-Type VMS Deposits of the Rudny Altai (Central Asia). Economic Geology, 2014, 109, 1403-1430.	3.8	34
86	Nature of assean lake ancient crust, Manitoba: a combined SHRIMP–ID-TIMS U–Pb geochronology and Sm–Nd isotope study. Precambrian Research, 2003, 126, 55-94.	2.7	33
87	U–Pb geochronology and Sr/Nd isotope compositions of groundmass perovskite from the newly discovered Jurassic Chidliak kimberlite field, Baffin Island, Canada. Earth and Planetary Science Letters, 2015, 415, 183-199.	4.4	33
88	Diamond ages from Victor (Superior Craton): Intra-mantle cycling of volatiles (C, N, S) during supercontinent reorganisation. Earth and Planetary Science Letters, 2018, 490, 77-87.	4.4	33
89	A Uâ€Pb zircon study of the Mesoproterozoic Charleston Granite, Gawler Craton, South Australia. Australian Journal of Earth Sciences, 1993, 40, 519-526.	1.0	31
90	Age and tectonomagmatic setting of the Eocene Çöpler–Kabataş magmatic complex and porphyry-epithermal Au deposit, East Central Anatolia, Turkey. Mineralium Deposita, 2013, 48, 557-583.	4.1	31

#	ARTICLE	IF	CITATIONS
91	Geochemical and Nd isotopic constraints for the origin of Late Archean turbidites from the Yellowknife area, Northwest Territories, Canada. Geochimica Et Cosmochimica Acta, 1999, 63, 2579-2598.	3.9	29
92	Multiple age components in individual molybdenite grains. Chemical Geology, 2012, 300-301, 55-60.	3.3	28
93	The Bear River dykes (1265–1269 Ma): westward continuation of the Mackenzie dyke swarm into Yukon, Canada. Precambrian Research, 2004, 133, 175-186.	2.7	27
94	The late- to postorogenic transition in the Neoproterozoic Agudos Grandes Granite Batholith (ApiaÃ) Tj ETQq0 0 0 American Earth Sciences, 2007, 23, 193-212.	rgBT /Ov 1.4	erlock 10 Tf 27
95	Formation of cratonic subcontinental lithospheric mantle and complementary komatiite from hybrid plume sources. Contributions To Mineralogy and Petrology, 2011, 161, 947-960.	3.1	27
96	The geochemical composition of serpentinites in the Mesoarchaean Tartoq Group, SW Greenland: Harzburgitic cumulates or melt-modified mantle?. Lithos, 2014, 198-199, 103-116.	1.4	27
97	The nature of Mesoarchaean seawater and continental weathering in 2.85 Ga banded iron formation, Slave craton, NW Canada. Geochimica Et Cosmochimica Acta, 2016, 194, 34-56.	3.9	27
98	Neodymium isotope geochemistry of felsic volcanic and intrusive rocks from the Yukon–Tanana Terrane in the Finlayson Lake Region, Yukon, Canada. Canadian Journal of Earth Sciences, 2003, 40, 77-97.	1.3	26
99	Re–Os and U–Pb constraints on gold mineralisation events in the Meso- to Neoarchaean StorÃ, greenstone belt, StorÃ, southern West Greenland. Precambrian Research, 2012, 200-203, 149-162.	2.7	26
100	Geology and Geochronology of the Golpu Porphyry and Wafi Epithermal Deposit, Morobe Province, Papua New Guinea. Economic Geology, 2018, 113, 271-294.	3.8	26
101	Petrogenesis and Magmatic Evolution of the Guichon Creek Batholith: Highland Valley Porphyry Cu ± (Mo) District, South-Central British Columbiaâ~¼. Economic Geology, 2017, 112, 1857-1888.	3.8	25
102	Geochronology of the Tumpangpitu Porphyry Au-Cu-Mo and High-Sulfidation Epithermal Au-Ag-Cu Deposit: Evidence for Pre- and Postmineralization Diatremes in the Tujuh Bukit District, Southeast Java, Indonesia. Economic Geology, 2018, 113, 163-192.	3.8	25
103	Sulphide Re-Os geochronology links orogenesis, salt and Cu-Co ores in the Central African Copperbelt. Scientific Reports, 2018, 8, 14946.	3.3	25
104	Understanding the microscale spatial distribution and mineralogical residency of Re in pyrite: Examples from carbonate-hosted Zn-Pb ores and implications for pyrite Re-Os geochronology. Chemical Geology, 2020, 533, 119427.	3.3	25
105	The origin of Triassic/Jurassic kimberlite magmatism, Canada: Two mantle sources revealed from the Sr-Nd isotopic composition of groundmass perovskite. Geochemistry, Geophysics, Geosystems, 2011, 12, n/a-n/a.	2.5	24
106	The Timing of Yellowknife Gold Mineralization: A Temporal Relationship with Crustal Anatexis?. Economic Geology, 2011, 106, 713-720.	3.8	24
107	Depositional age of the early Paleoproterozoic Klipputs Member, Nelani Formation (Ghaap Group,) Tj ETQq1 1 0.74 Paleoproterozoic global correlations. Precambrian Research, 2013, 237, 1-12.	84314 rgE 2.7	3T /Overlock 24
108	The origin of Late Devonian (Frasnian) stratiform and stratabound mudstone-hosted barite in the Selwyn Basin, Northwest Territories, Canada. Marine and Petroleum Geology, 2017, 85, 1-15.	3.3	24

#	Article	IF	CITATIONS
109	Integrated Nd isotopic and U–Pb detrital zircon systematics of clastic sedimentary rocks from the Slave Province, Canada: evidence for extensive crustal reworking in the early- to mid-Archean. Earth and Planetary Science Letters, 2000, 174, 283-299.	4.4	23
110	Synvolcanic and Younger Plutonic Rocks from the Blake River Group: Implications for Regional Metallogenesis. Economic Geology, 2008, 103, 1243-1268.	3.8	23
111	The Carolina kimberlite, Brazil — Insights into an unconventional diamond deposit. Lithos, 2009, 112, 843-851.	1.4	23
112	Timing and thermochemical constraints on multi-element mineralisation at the Nori/RA Cu–Mo–U prospect, Great Bear magmatic zone, Northwest Territories, Canada. Mineralium Deposita, 2010, 45, 549-566.	4.1	23
113	Eocambrian granite clasts in southern British Columbia shed light on Cordilleran hinterland crust. Canadian Journal of Earth Sciences, 2001, 38, 1007-1016.	1.3	22
114	Extending the ancient margin outboard in the Canadian Cordillera: record of Proterozoic crust and Paleocene regional metamorphism in the Nicola horst, southern British Columbia. Canadian Journal of Earth Sciences, 2002, 39, 1605-1623.	1.3	22
115	An Example of Synorogenic Sediment-Hosted Copper Mineralization: Geologic and Geochronologic Evidence from the Paleoproterozoic Nussir Deposit, Finnmark, Arctic Norway. Economic Geology, 2015, 110, 677-689.	3.8	21
116	Evidence for a nonmagmatic component in potassic hydrothermal fluids of porphyry cu-Au-Mo systems, Yukon, Canada. Geochimica Et Cosmochimica Acta, 2001, 65, 571-587.	3.9	20
117	Temporal Evolution of the Western Porphyry Cu-Au Systems at Reko Diq, Balochistan, Western Pakistan. Economic Geology, 2014, 109, 2003-2021.	3.8	20
118	Tectonic Triggers for Postsubduction Magmatic-Hydrothermal Gold Metallogeny in the Late Cenozoic Anatolian Metallogenic Trend, Turkey. Economic Geology, 2019, 114, 1339-1363.	3.8	20
119	Origin and evolution of mid- to late-Archean crust in the Hanikahimajuk Lake area, Slave Province, Canada; evidence from U–Pb geochronological, geochemical and Nd–Pb isotopic data. Precambrian Research, 2000, 99, 197-224.	2.7	19
120	Radiogenic isotope characteristics of the Mesoproterozoic intrusive rocks of the Nipigon Embayment, northwestern Ontario. Canadian Journal of Earth Sciences, 2007, 44, 1111-1129.	1.3	19
121	The Churchill kimberlite field, Nunavut, Canada: petrography, mineral chemistry, and geochronology. Canadian Journal of Earth Sciences, 2008, 45, 1039-1059.	1.3	19
122	Re-Os geochronological constraints on the mineralizing events within the Mount Pleasant Caldera: implications for the timing of sub-volcanic magmatism. Atlantic Geology, 0, 49, 131.	0.2	19
123	The Mesoproterozoic Abra polymetallic sedimentary rock-hosted mineral deposit, Edmund Basin, Western Australia. Ore Geology Reviews, 2016, 76, 442-462.	2.7	19
124	Temporal evolution of mineralization events in the Bohemian Massif inferred from the Re–Os geochronology of molybdenite. Mineralium Deposita, 2017, 52, 651-662.	4.1	18
125	Sm–Nd fluorite dating of Proterozoic low-sulfidation epithermal Au–Ag deposits and U–Pb zircon dating of host rocks at Mallery Lake, Nunavut, Canada. Canadian Journal of Earth Sciences, 2003, 40, 1789-1804.	1.3	17
126	The High-Grade Mo-Re Merlin Deposit, Cloncurry District, Australia: Paragenesis and Geochronology of Hydrothermal Alteration and Ore Formation. Economic Geology, 2017, 112, 397-422.	3.8	17

#	Article	IF	CITATIONS
127	Provenance of Jurassic sedimentary rocks of south-central Quesnellia, British Columbia: implications for paleogeography. Canadian Journal of Earth Sciences, 2004, 41, 103-125.	1.3	16
128	Linking the Timing of Disseminated Granite-Hosted Gold-Rich Deposits to Paleoproterozoic Felsic Magmatism at Alta Floresta Gold Province, Amazon Craton, Brazil: Insights from Pyrite and Molybdenite Re-Os Geochronology. Economic Geology, 2017, 112, 1937-1957.	3.8	16
129	Domestic cattle mobility in early farming villages in southern Africa: harvest profiles and strontium (87Sr/86Sr) isotope analyses from Early Iron Age sites in the lower Thukela River Valley of South Africa. Archaeological and Anthropological Sciences, 2013, 5, 129-144.	1.8	15
130	Radiogenic isotope chemostratigraphy reveals marine and nonmarine depositional environments in the late Mesoproterozoic Borden Basin, Arctic Canada. Bulletin of the Geological Society of America, 2019, 131, 1965-1978.	3.3	15
131	Granulite sulphides as tracers of lower crustal origin and evolution: An example from the Slave craton, Canada. Geochimica Et Cosmochimica Acta, 2010, 74, 5368-5381.	3.9	14
132	Lithosphere-asthenosphere mixing in a transform-dominated late Paleozoic backarc basin: Implications for northern Cordilleran crustal growth and assembly. , 2012, 8, 716-739.		14
133	The late Oligocene Cevizlidere Cu-Au-Mo deposit, Tunceli Province, eastern Turkey. Mineralium Deposita, 2015, 50, 245-263.	4.1	14
134	Re-Os Systematics of Löllingite and Arsenopyrite In Granulite-Facies Garnet Rocks: Insights Into the Metamorphic History and Thermal Evolution of the Broken Hill Block During the Early Mesoproterozoic (New South Wales, Australia). Canadian Mineralogist, 2017, 55, 29-44.	1.0	14
135	The Tongkuangyu Cu Deposit, Trans-North China Orogen: A Metamorphosed Paleoproterozoic Porphyry Cu Deposit. Economic Geology, 2020, 115, 51-77.	3.8	14
136	Detrital zircon geochronology and provenance of Late Proterozoic and mid-Paleozoic successions outboard of the miogeocline, southeastern Canadian Cordillera. Canadian Journal of Earth Sciences, 2007, 44, 1675-1693.	1.3	13
137	Meso- and Neoarchean evolution of the Island Lake greenstone belt and the northwestern Superior Province: Evidence from lithogeochemistry, Nd isotope data, and U–Pb zircon geochronology. Precambrian Research, 2014, 246, 160-179.	2.7	13
138	SQUAW PEAK, ARIZONA: PALEOPROTEROZOIC PRECURSOR TO THE LARAMIDE PORPHYRY COPPER PROVINCE. Economic Geology, 2014, 109, 1171-1177.	3.8	12
139	Athapuscow aulacogen revisited: Geochronology and geochemistry of the 2046â€⁻Ma Union Island Group mafic magmatism, East Arm of Great Slave Lake, Northwest Territories, Canada. Precambrian Research, 2019, 321, 85-102.	2.7	12
140	Magmatic and structural controls on porphyry-style Cu–Au–Mo mineralization at Kemess South, Toodoggone District of British Columbia, Canada. Mineralium Deposita, 2009, 44, 435-462.	4.1	11
141	Geology and Genesis of the Cerro la Mina Porphyry-High Sulfidation Au (Cu-Mo) Prospect, Mexico. Economic Geology, 2017, 112, 799-827.	3.8	11
142	The Mineralogical Evolution of the Clastic Dominant-Type Zn-Pb ± Ba Deposits at Macmillan Pass (Yukon, Canada)—Tracing Subseafloor Barite Replacement in the Layered Mineralization. Economic Geology, 2020, 115, 961-979.	3.8	11
143	Biomass-Derived Provenance Dominates Glacial Surface Organic Carbon in the Western Himalaya. Environmental Science & Technology, 2020, 54, 8612-8621.	10.0	11
144	Osmium isotopic constraints on sulphide formation in the epithermal environment of magmatic-hydrothermal mineral deposits. Chemical Geology, 2021, 564, 120053.	3.3	11

#	Article	IF	CITATIONS
145	Crustal recycling during subduction at the Eocene Cordilleran margin of North America: a petrogenetic study from the southwestern Yukon. Canadian Journal of Earth Sciences, 2003, 40, 1805-1821.	1.3	10
146	Assimilation, differentiation, and thickening during formation of arc crust in space and time: The Jurassic Bonanza arc, Vancouver Island, Canada. Bulletin of the Geological Society of America, 2016, 128, 543-557.	3.3	10
147	Reply to discussions of "Age of the Zambian Copperbelt―by Hitzman and Broughton and Muchez et al Mineralium Deposita, 2017, 52, 1277-1281.	4.1	10
148	Carmacks Copper Cu-Au-Ag Deposit: Mineralization and Postore Migmatization of a Stikine Arc Porphyry Copper System in Yukon, Canada. Economic Geology, 2020, 115, 1413-1442.	3.8	10
149	The late- to postorogenic transition in the ApiaÃ-domain, SE Brazil: Constraints from the petrogenesis of the Neoproterozoic Agudos Grandes Granite Batholith. Journal of South American Earth Sciences, 2007, 23, 213-235.	1.4	9
150	Genesis of the Au–Bi–Cu–As, Cu–Mo ± W, and base–metal Au–Ag mineralization at the M Freegold (Yukon, Canada): constraints from Ar–Ar and Re–Os geochronology and Pb and stable isotope compositions. Mineralium Deposita, 2013, 48, 991-1017.	lountain 4.1	9
151	Preservation of Reâ€Os isotope signatures in pyrite throughout lowâ€ <i>T</i> , highâ€ <i>P</i> eclogite facies metamorphism. Terra Nova, 2014, 26, 402-407.	2.1	9
152	Characterising the southern part of the Hearne Province: A forgotten part of Canada's shield revisited. Precambrian Research, 2018, 307, 51-65.	2.7	9
153	Sm-Nd Isotope Technique as An Exploration Tool: Delineating the Northern Extension of the Thompson Nickel Belt, Manitoba, Canada. Economic Geology, 2007, 102, 1217-1231.	3.8	8
154	Re-Os MOLYBDENITE AGES FROM THE ARCHEAN YELLOWKNIFE GREENSTONE BELT: COMPARISON TO U-Pb AGES AND EVIDENCE FOR METAL INTRODUCTION AT Â2675 Ma. Economic Geology, 2007, 102, 511-518.	3.8	7
155	A petrological and geochronological study of a 360 Ma metallogenic event in Maritime Canada with implications for lithophile-metal mineralization in the Canadian Appalachians. Canadian Journal of Earth Sciences, 2013, 50, 1147-1163.	1.3	7
156	Retrogression of eclogite-facies shear zones by short-lived fluid infiltration during the Caledonian orogeny, Lofoten islands, Norway. Geological Society Special Publication, 2014, 390, 443-466.	1.3	7
157	Implications of high-precision Re-Os molybdenite dating of the Navachab orogenic gold deposit, Namibia. Geochemistry: Exploration, Environment, Analysis, 2015, 15, 125-130.	0.9	7
158	Geologic History and Timing of Mineralization at the Haile Gold Mine, South Carolina. Economic Geology, 2014, 109, 1863-1881.	3.8	6
159	Elemental and isotopic compositions of trench-slope black shales, Bohemian Massif, with implications for oceanic and atmospheric oxygenation in early Cambrian. Palaeogeography, Palaeoclimatology, Palaeoecology, 2021, 564, 110195.	2.3	6
160	lsotopic Re-Os age of molybdenite from the Szklarska Poręba Huta Quarry (Karkonosze, SW Poland). Geological Quarterly, 2012, 56, 505-512.	0.2	6
161	Re-Os systematics and chronology of graphite. Geochimica Et Cosmochimica Acta, 2022, 323, 164-182.	3.9	6
162	A petrological and geochemical study of the volcanic rocks of the Crowsnest Formation, southwestern Alberta, and of the Howell Creek suite, British Columbia. Canadian Journal of Earth Sciences, 2006, 43, 1621-1637.	1.3	5

#	Article	IF	CITATIONS
163	Rb–Sr and U–Pb geochronology and setting of the Buffalo Head Hills kimberlite field, northern AlbertaThis article is one of a selection of papers published in this Special Issue on the theme <i>Geology of northeastern British Columbia and northwestern Alberta: diamonds, shallow gas, gravel, and glaciers</i> Canadian Journal of Earth Sciences, 2008, 45, 513-529.	1.3	5
164	ROSEN, BULGARIA: A NEWLY RECOGNIZED IRON OXIDE-COPPER-GOLD DISTRICT. Economic Geology, 2020, 115, 481-488.	3.8	5
165	Comment and Reply on "A-type granites revisited: Assessment of a residual-source model". Geology, 1991, 19, 1151.	4.4	4
166	Mississippian volcanic assemblage conformably overlying Cordilleran miogeoclinal strata, Turnagain River area, northern British Columbia, is not part of an accreted terrane. Canadian Journal of Earth Sciences, 2005, 42, 1449-1465.	1.3	4
167	Correlation of mid-Cretaceous granites with source terranes in the northern Canadian CordilleraLithoprobe Publication 1475 Canadian Journal of Earth Sciences, 2008, 45, 389-403.	1.3	4
168	Mesoproterozoic porphyry copper mineralization at Mamainse Point, Ontario, Canada in the context of Midcontinent rift metallogeny. Ore Geology Reviews, 2020, 127, 103831.	2.7	4
169	Genetic link between gold mineralization and porphyry magmatism in the Baogutu district, West Junggar, NW China: Constraints from Reâ€Os and S isotopes in sulphide. Geological Journal, 2020, 55, 6098-6105.	1.3	4
170	The Evolution and Structural Modification of the Supergiant Mitchell Au-Cu Porphyry, Northwestern British Columbia. Economic Geology, 2019, 114, 303-324.	3.8	3
171	High-precision ReOs dating of Lower Jurassic shale packages from the Western Canadian Sedimentary Basin. Palaeogeography, Palaeoclimatology, Palaeoecology, 2020, 560, 110010.	2.3	3
172	The Productora Cu-Au-Mo Deposit, Chile: A Mesozoic Magmatic-Hydrothermal Breccia Complex with Both Porphyry and Iron Oxide Cu-Au Affinities. Economic Geology, 2020, 115, 543-580.	3.8	3
173	Geology and resource development of the Kelvin kimberlite pipe, Northwest Territories, Canada. Mineralogy and Petrology, 2018, 112, 463-475.	1.1	2
174	Chronology of the Kašperské Hory orogenic gold deposit, Bohemian Massif, Czech Republic. Mineralium Deposita, 2019, 54, 473-484.	4.1	2
175	On the timing and metallogenic implications of the sediment-hosted stratiform copper–silver mineralization in the Creston Formation (Belt-Purcell Supergroup), British Columbia, Canada. Ore Geology Reviews, 2021, 131, 104032.	2.7	2
176	Synsedimentary to Diagenetic Cu±Co Mineralization in Mesoproterozoic Pyritic Shale Driven by Magmatic-Hydrothermal Activity on the Edge of the Great Falls Tectonic Zone–Black Butte, Helena Embayment, Belt-Purcell Basin, USA: Evidence from Sulfide Re-Os Isotope Geochemistry. Lithosphere, 2021, 2021, .	1.4	2
177	Comment and Reply on "Depth and mineralogy of the magma source or pause region for the Carboniferous Liberty Hill pluton, South Carolina". Geology, 1989, 17, 482.	4.4	1
178	Metallogeny of the Marco zone, Corvet Est, disseminated gold deposit, James Bay, Quebec, Canada. Canadian Journal of Earth Sciences, 2012, 49, 1154-1176.	1.3	1
179	Geology and age of the Morrison porphyry Cu–Au–Mo deposit, Babine Lake area, British Columbia. Canadian Journal of Earth Sciences, 2016, 53, 950-978.	1.3	1
180	Crustal Sulfide Minerals (Re-Os). Encyclopedia of Earth Sciences Series, 2015, , 191-196.	0.1	1

#	Article	IF	CITATIONS
181	Lufilian copper–gold mineralization in the Mkushi District, Zambia: regional metallogenic implications. Mineralium Deposita, 0, , 1.	4.1	1
182	Constraints on the timing of Marinoan ?Snowball Earth? glaciation by 187Re?187Os dating of a Neoproterozoic, post-glacial black shale in Western Canada. Earth and Planetary Science Letters, 2004, 222, 729-729.	4.4	0
183	Crustal Sulfide Minerals (Re-Os). , 2014, , 1-8.		0
184	Multiphase formation of the ObÅ™Ã-dÅ⁻l polymetallic skarn deposit, West Sudetes, Bohemian Massif: geochemistry and Re–Os dating of sulfide mineralization. Mineralium Deposita, 2018, 53, 665-682.	4.1	0